Risk of multiple interacting tipping points should encourage rapid CO_2 emission reduction

Yongyang Cai[1,2]*, Timothy M. Lenton[3]*, Thomas S. Lontzek[4]*

*All authors contributed equally to this work

[1]Hoover Institution, Stanford University, Stanford, CA 94305, USA

[2]Becker Friedman Institute, University of Chicago, Chicago, IL 60636, USA

[3]College of Life and Environmental Sciences, University of Exeter, Exeter EX4 4QE, UK

[4]Department of Quantitative Business Administration, University of Zurich, 8008 Zürich, CH

Evidence suggests that several elements of the climate system could be tipped into a different state by global warming, causing irreversible economic damages. To address their policy implications, we incorporated five interacting climate tipping points into a stochastic-dynamic integrated assessment model, calibrating their likelihoods and interactions on results from an existing expert elicitation. Here we show that combining realistic assumptions about policymaker's preferences under uncertainty, with the prospect of multiple future interacting climate tipping points, increases the present social cost of carbon (SCC) in the model nearly 8-fold from \$15/tCO_2 to \$116/tCO_2. Furthermore, passing some tipping points increases the likelihood of other tipping points occurring to such an extent that it abruptly increases the social cost of carbon. The corresponding optimal policy involves an immediate, massive effort to control CO_2 emissions, which are stopped by mid-century, leading to climate stabilization at <1.5 °C warming above pre-industrial levels.

The social cost of carbon (SCC) represents the cost of all future climate damages stemming from a marginal emission of CO_2, discounted to the year of emission. The 2010 US Federal assessment[1] used three simple integrated assessment models (IAMs) to arrive at a SCC of \$21/tCO_2 for a tonne emitted in 2010, which was subsequently revised upwards[2] to \$33/tCO_2. Several other studies[3-6] have argued for a higher SCC on various grounds. A key potential contributor to increasing the SCC is the possibility that ongoing climate change will cause elements of the climate system to pass 'tipping points' leading to irreversible damages[7,8].

Existing scientific studies suggest there are multiple climate tipping points that could be triggered this century or next if climate change continues unabated[7,8], and there are causal interactions between tipping events such that tipping one element affects the likelihoods of tipping others[8] (Fig. 1). The likelihood of specific tipping events varies, but is generally expected to increase with global temperature[7,8]. However, internal variability within the climate system, and relatively rapid anthropogenic forcing, mean that even if deterministic tipping points could be precisely identified, the actual systems could be tipped earlier or later[9]. Thus, any assessment of their policy implications needs to represent the stochastic uncertainty surrounding when tipping points could occur[10]. Furthermore, the impacts of passing different tipping points are expected to vary[7,11], and to unfold at different rates depending on the internal timescale of the part of the climate system being tipped[7,11].

Relative to this scientific understanding, most cost-benefit analyses of climate change only allow for simple and scientifically unrealistic representations of climate tipping points[11]. Most previous IAM studies of climate catastrophes have treated them in a deterministic fashion, sometimes giving them a probability distribution[5,12-15]. Some recent IAM studies have considered one stochastic climate tipping point impacting economic output[10], non-market welfare[16], climate sensitivity[17], or carbon cycle feedbacks[17]. This can lead to up to 200% increases in the SCC in extreme cases[10], with the results clearly sensitive to the timescale over which tipping point impacts unfold, as well as the final magnitude of those impacts[10]. However, there has been little consideration of multiple tipping points and interactions between them, or of how an appropriate representation of risk aversion affects the optimal response to the prospect of future tipping points.

A recent IAM study[18] has examined three loosely-defined tipping points that instantaneously alter climate sensitivity, carbon cycle feedbacks, or economic output, and interact via their effects on atmospheric CO_2, global temperature, or economic output. Here we consider five carefully-defined tipping points[7,8] and the direct causal interactions between them identified by scientific experts[8] (Fig. 1). These interactions occur primarily via aspects of the climate system that are not resolved in simple IAMs. The impacts of our tipping points unfold at a rate appropriate for the system being tipped, in contrast with instantaneous changes[17,18] in climate sensitivity and carbon cycle feedbacks which are scientifically questionable[10]. Our tipping points principally affect economic output, although we also consider their feedback effects on the carbon cycle. Instead of arbitrarily specifying the likelihood of the tipping points[18] we calibrate their likelihoods (and the causal interactions between them) based on the results of an existing expert elicitation[8]. Furthermore, in contrast to recent work[18], we alter the specification of the social planner’s preferences regarding risk aversion and intergenerational equity, in a manner appropriate for the stochastic uncertainty surrounding future tipping points.

Modelling tipping points

We use the dynamic stochastic integration of climate and economy (DSICE) framework[19] to incorporate five stochastic tipping points and causal interactions between them into the 2013 version of the well-known DICE model[20] (see Methods, Supplementary Figs. 1,2). This means solving a 16-dimensional stochastic model – the first time in the field of economics of climate change that an analysis on such a scale has been accomplished (our previous work[10] solved a 7-dimensional system, whereas other simplified stochastic versions[17] of DICE only consider 4 dimensions). In our stochastic version of the DICE model, we use annual time steps, and calibrate parameters in the carbon cycle and temperature modules against the emulated median response of complex climate models for the four RCP (representative concentration pathway) scenarios[21] (see Supplementary Methods). In a deterministic setting within our model (without considering climate tipping points) our calibration gives a social cost of carbon in 2010 of \$15/tCO_2 (all results are in 2010 US dollars). For reference, Nordhaus' DICE-2013R model[20] which uses five-year time steps and is calibrated against one RCP scenario also has a 2010 SCC of \$15/tCO_2.

In IAMs such as DICE, greater emission control at present mitigates damages from climate change in the future but limits consumption and/or capital investment today. A 'social planner' is assumed to weigh these costs and benefits of emission control to maximize the expected present value of global social welfare. When faced with stochastic uncertainty about future tipping events, the social planner's response will depend on their preferences regarding risk and smoothing consumption. DICE adopts a specification of risk aversion that is inversely tied to the decision maker's preferences to smooth consumption over time (i.e. the inter-temporal elasticity of substitution). Thus, a high inter-temporal elasticity of substitution is taken to imply a low risk aversion. In the baseline DICE model, risk aversion RA=1.45, and inter-temporal elasticity of substitution IES=1/1.45. However, empirical economic data do not support this inverse proportionality (implying time separable utility) and suggest instead decoupling these preferences[22]. Hence we incorporated 'Epstein-Zin' (EZ) preferences[22] using default parameter settings[23] of RA=3.066 and IES=1.5, which are consistent with empirical findings[23] (implying time non-separable utility). Estimates of IES>1 have been obtained from e.g. stockholder data[24], IES=1.5 is used in a long-run risk model[19,25], and the upper bound is considered[23] to be IES ~2. Using IES=1.5, equity returns data[23] suggest RA=3.066, which is in the range RA=3-4 from a separate study of equity premiums of rare disasters[26], with the upper bound considered[25] to be RA~10.

The five interacting, stochastic, potential climate tipping points[7,8] (Fig. 1, Table 1) represent reorganisation of the Atlantic Meridional Overturning Circulation (AMOC), disintegration of the Greenland Ice Sheet (GIS), collapse of the West Antarctic Ice Sheet (WAIS), dieback of the Amazon rainforest (AMAZ), and shift to a more persistent El-Niño regime (ENSO). We used published expert elicitation results[8] to derive the likelihoods (see Methods) of each of the five tipping events (Table 1), and the causal interactions between them (Fig. 1, Supplementary Table 1). By causal interaction we mean that the hazard rate of each tipping point depends on the state of the others.

For each tipping event we specified a transition timescale[10] (Table 1, see Methods) – i.e. how long it would take for the full impacts to unfold, based on current scientific understanding of the timescales of the systems being tipped[7,11] (e.g. ice sheets melt more slowly than the ocean circulation can reorganise). Recognising the scientific uncertainty surrounding transition times we explore a factor of 5 uncertainty range in either direction. We must also specify a final damage for each tipping event (Table 1, see Methods), taken to be an irreversible percentage reduction in world GDP. This is the most problematic and debatable part of the parameterisation, because of a gross shortage of scientific and economic estimates of tipping point damages[11]. We can make some scientific inferences about relative damages (e.g. based on the eventual contributions of different ice sheets to sea-level rise). Past studies with DICE have loosely associated a 25-30% reduction in GDP comparable with the Great Depression with a collapse of the AMOC[27,28], but when combined with other tipping points this could lead to excessively high overall damages. Our assigned damages for individual tipping points range from 5-15% reduction in GDP with a combined reduction in GDP if all five tipping events occur and complete their transitions of 38%. However, due to relatively low probabilities and long transition timescales, the expected tipping point damages in our default scenario only amount to 0.53% of GDP in 2100 and 1.89% of GDP in 2200. In our sensitivity analysis we consider a factor of 2-3 total uncertainty range in final damages for each tipping point. Finally, we include some conservative effects of tipping particular systems on the carbon cycle (Table 1, see Methods).

Optimal policy

The result of including multiple interacting tipping points under EZ preferences (Fig. 2) is a nearly 8-fold increase in the initial social cost of carbon from \$15/tCO_2 in the baseline model (grey line) to \$116/tCO_2 (black line). Across 10,000 sample paths of the model there are cases where one or more tipping points still occur, leading to uncertainty ranges for the key variables (grey shaded areas). The emissions control rate jumps from ~18% to ~56% in 2010 and rises to 100% by 2050, effectively shutting down fossil fuel CO_2 emissions – whereas in the baseline model emissions continue into the next the century. The average atmospheric carbon peaks in the 2030s at 415 ppm and then declines (due to ongoing ocean carbon uptake) – whereas in the baseline model atmospheric CO_2 continues to rise to ~650 ppm by 2100. Temperature rise slows down and is almost stable around 1.4 °C above pre-industrial by 2100 – whereas in the baseline model warming continues and approaches 3 °C by 2100. Following the expected path (black line) there is only an 11% probability of one or more tipping events by 2100, reduced from 46% in the baseline model, or 87% under a prescribed RCP8.5 emissions scenario (Table 2).

A factor of 2.4 increase from the baseline SCC to \$36/tCO_2 is just due to the change to EZ preferences (dashed black line, Fig. 2), with a further factor of 3.2 increase due to the potential for multiple tipping points. With just EZ preferences (and no stochastic tipping points) the initial emissions control rate increases from ~18% to ~29% with 100% emissions control in 2100. Atmospheric carbon peaks around 550 ppm, with surface temperature stabilising around 2.3 °C above pre-industrial.

Tipping point interactions

In the full model, there are both positive and negative causal interactions between tipping points (Fig. 1, Supplementary Table 1), which are conservatively calibrated (see Methods). Hence their inclusion has only a modest net effect on the expected SCC, increasing it from \$109/tCO_2 to \$116/tCO_2 (see also Supplementary Fig. 3). However, a specific sample path where multiple tipping events occur before 2200 (Fig. 3, solid line) reveals that some tipping point interactions can have a strong effect on the time evolution of the SCC. Considering a no interactions sample path (Fig. 3, dashed line) shows that in general, passing a tipping point reduces the incentive to mitigate and therefore lowers the SCC, because it can no longer be avoided. However, with interactions, tipping of the GIS significantly increases the likelihood of AMOC tipping (which is assumed to be the most damaging event) hence this causes a large increase in the SCC in order to try to avoid AMOC tipping. (This is consistent with previous suggestions[29,30] that tipping points can create multiple optima – here for the SCC and corresponding emissions[30].) Subsequent tipping of AMOC greatly reduces the SCC. Tipping of ENSO causes a small increase in the SCC because it increases the likelihood of tipping the Amazon. Subsequent tipping of the Amazon halves the SCC because there is now an unavoidable extra source of carbon to the atmosphere and only WAIS left to tip. There are other sample paths where the first tipping event does not increase the likelihood of others so the SCC drops – e.g. when the Amazon rainforest tips first (Supplementary Fig. 4).

The social cost of carbon therefore depends on whether tipping events occur and in which order. This can also be seen by looking at the sample paths for the earliest and sole tipping before 2100 of each element (Supplementary Fig. 5). If the GIS tips first this leads to the highest SCC path and the most stringent emission control, reaching 100% before 2040, because of the increased risk of AMOC collapse. If the AMOC tips first, this gives the lowest SCC path because it has the greatest damages, which can no longer be avoided – yet emission control remains above 60% and the SCC remains above \$110/tCO_2. If the Amazon tips first, this also lowers SCC and emission control, but it leads to the highest atmospheric carbon and temperature trajectory because of an accompanying carbon source. If ENSO tips first, this slightly increases emission control because the likelihood of the AMAZ tipping is increased. If the WAIS tips first, there is little effect on emission control because it only slightly increases the likelihood of tipping the AMOC and GIS. CO_2 emissions trajectories (Supplementary Fig. 6) therefore depend on the contemporaneous state of tipping elements.

Sensitivity analysis

The high social cost of carbon is robust to sensitivity analyses (see Methods). Combined variations in assumed transition times and final damages of the tipping points give a full range in initial SCC of \$50-166/tCO_2 (Supplementary Table 2). With pessimistic settings for the expert assessment of interactions between tipping elements (Supplementary Table 3), the SCC increases from \$116/tCO_2 to \$121/tCO_2. Including an endogenous transition time for the GIS gives only a slight reduction in SCC to \$114/tCO_2 because its damages tend to be discounted away anyway. Allowing all tipping elements to have an endogenous transition time reduces SCC to \$94/tCO_2.

Retaining an intertemporal elasticity of substitution IES=1.5 but increasing risk aversion to RA=10 increases the SCC from \$116/tCO_2 to \$146/tCO_2. With the original RA=3.066 and an upper limit of IES=2 the SCC increases to \$151/tCO_2. Using the default DICE settings of IES=1/1.45 and RA=1.45 gives an SCC of \$28/tCO_2, a factor 1.9 increase from the default \$15/tCO_2 due to the five interacting tipping points. Thus, EZ preferences magnify the effect of including potential future tipping points, causing a factor 3.2 (rather than 1.9) increase in the SCC. To disentangle the effect of IES and RA, we also investigate a case with IES=1.5 and RA=1/1.5, which gives an SCC of \$104/tCO_2. That is, when we incorporate the climate tipping risks, using time separable preferences as in DICE, an increase from IES=1/1.45 (and RA=1.45) to IES=1.5 (and RA=1/1.5) leads to a factor 3.7 increase in the SCC, and the additional change to our default time non-separable EZ preferences (IES=1.5, RA=3.066) leads to an extra SCC of \$12/tCO_2.

Discussion and conclusion

Putting our results in scientific context, there is already evidence that major ice sheets are losing mass at an accelerating rate[31,32]. GIS mass loss is estimated to be contributing ~0.7 mm/yr to sea-level rise[33], with a corresponding increase in freshwater flux to the North Atlantic[34] since 1990 of ~0.01 Sv. Although modest at present, this and other contributors to increasing freshwater input to the North Atlantic[35], are thought[8] to increase the likelihood of AMOC tipping, and our results suggest this should be increasing the incentive to control CO_2 emissions. WAIS mass loss is contributing ~0.35 mm/yr to sea-level rise[32], and there is evidence that parts of the West Antarctic ice sheet are already in irreversible retreat[36-38]. If the

WAIS has already passed a tipping point then mitigation cannot avoid it, but our results suggest this should not significantly reduce the incentive to mitigate to try to avoid other tipping events.

Our results and policy recommendations differ considerably from another recent study considering multiple tipping points[18], which recommends at most a doubling of the social cost of carbon (SCC) that allows CO_2 emissions to continue to grow past mid-century, with temperature ultimately peaking at just under 3 °C. In contrast, our results recommend a nearly 8-fold increase in the SCC to drive a cessation of CO_2 emissions by mid-century, which limits warming to <1.5 °C. This very different outcome is a result of our different specification of tipping points together with our change in decision maker preferences to something more appropriate for such stochastic climate risks.

There are several caveats with the DICE modelling approach used here (and the simplified version of DICE used elsewhere[18]). In the climate component of the model, the ocean carbon sink is too strong[39], causing it to overestimate the effect of emissions reductions on atmospheric CO_2 and temperature, especially beyond 2100. We only consider one value for equilibrium climate sensitivity (2.9 °C following DICE-2013), whereas the IPCC likely range[40] spans 1.5-4.5 °C. Nevertheless, the DICE prediction that a shut-down of CO_2 emissions by mid-century will lead to ~1.5 °C warming, is compatible with more detailed probabilistic projections[41,42] varying climate sensitivity (noting that DICE shuts down emission faster but then does not allow for net carbon dioxide removal in the second half of this century[41,42]).

The economic component of DICE allows for an unrealistic instantaneous adjustment of emissions (to e.g. a control rate >0.5), whereas in reality emissions control rates are low and there are lags in ramping them up, for example due to the lifetime of coal-fired power stations. However, recent energy-economic model studies[41,42] show that it is technologically feasible to increase the emissions control rate to 100%, and thus achieve net zero CO_2 emissions, by mid-century. The assumed costs of mitigation options in DICE are also relatively low[43], whereas energy-economic models[41] indicate that limiting warming to 1.5 °C would be considerably more expensive than limiting it to 2 °C, especially between now and 2030. Despite these uncertainties, in a real options analysis framework[44], paying up front now to minimise the future risk of climate tipping points can still be the logical and cost-effective option for societies. Furthermore, acknowledging that society also faces other potential tipping points (e.g. disease pandemics) should increase the willingness to pay to avert any one of them[45], even though we should not necessarily avert all of them[45]. The decision to try to avert climate tipping points depends crucially on a relatively high risk aversion[45], consistent with our findings.

In summary, our results illustrate that the prospect of multiple interacting climate tipping points with irreversible economic damages ought to be provoking very strong mitigation action, on the part of ‘social planners’ – including governments signed up to the United Nations Framework Convention on Climate Change. Under realistic preferences under uncertainty, the optimal policy involves a shutdown of carbon emissions by mid-century.

References

1 Interagency Working Group on Social Cost of Carbon, Social Cost of Carbon for Regulatory Impact Analysis - Under Executive Order 12866. United States Government, 2010.

2 Interagency Working Group on Social Cost of Carbon, Technical Update of the Social Cost of Carbon for Regulatory Impact Analysis. United States Government, 2013.

3 Dietz, S., High impact, low probability? An empirical analysis of risk in the economics of climate change. *Climatic Change* 108, 519-541 (2011).

4 Kopp, R.E., Golub, A., Keohane, N.O., & Onda, C., The Influence of the Specification of Climate Change Damages on the Social Cost of Carbon. *Economics: The Open-Access, Open-Assessment E-Journal* 6 (2012-13), 1-40 (2012).

5 Ackerman, F. & Stanton, E.A., Climate Risks and Carbon Prices: Revising the Social Cost of Carbon *Economics: The Open-Access, Open Assessment E-Journal* 6 (2012-10), 1-25 (2012).

6 van den Bergh, J.C.J.M. & Botzen, W.J.W., A lower bound to the social cost of CO2 emissions. *Nature Clim. Change* 4 (4), 253-258 (2014).

7 Lenton, T.M. *et al.*, Tipping Elements in the Earth's Climate System. *Proceedings of the National Academy of Sciences* 105 (6), 1786-1793 (2008).

8 Kriegler, E., Hall, J.W., Held, H., Dawson, R., & Schellnhuber, H.J., Imprecise probability assessment of tipping points in the climate system. *PNAS* 106 (13), 5041-5046 (2009).

9 Lenton, T.M., Early warning of climate tipping points. *Nature Climate Change* 1, 201-209 (2011).

10 Lontzek, T.S., Cai, Y., Judd, K.L., & Lenton, T.M., Stochastic integrated assessment of climate tipping points indicates the need for strict climate policy. *Nature Climate Change* 5 (4), 441-444 (2015).

11 Lenton, T.M. & Ciscar, J.-C., Integrating tipping points into climate impact assessments. *Climatic Change* 117 (3), 585-597 (2013).

12 Mastrandrea, M.D. & Schneider, S.H., Probabilistic Integrated Assessment of "Dangerous" Climate Change. *Science* 304 (5670), 571-575 (2004).

13 Kosugi, T., Integrated Assessment for Setting Greenhouse Gas Emission Targets under the Condition of Great Uncertainty about the Probability and Impact of Abrupt Climate Change. *Journal of Environmental Informatics* 14 (2), 89-99 (2009).

14 Ackerman, F., Stanton, E.A., & Bueno, R., Fat tails, exponents, extreme uncertainty: Simulating catastrophe in DICE. *Ecological Economics* 69 (8), 1657-1665 (2010).

15 Weitzman, M.L., GHG Targets as Insurance Against Catastrophic Climate Damages. *Journal of Public Economic Theory* 14 (2), 221-244 (2012).

16 Cai, Y., Judd, K.L., Lenton, T.M., Lontzek, T.S., & Narita, D., Environmental tipping points significantly affect the cost–benefit assessment of climate policies. *Proceedings of the National Academy of Sciences* 112 (15), 4606-4611 (2015).

17 Lemoine, D. & Traeger, C., Watch Your Step: Optimal Policy in a Tipping Climate. *American Economic Journal: Economic Policy* 6 (1), 137-166 (2014).

18 Lemoine, D. & Traeger, C.P., The Economics of Tipping the Climate Dominoes. *Nature Climate Change* (in press).

19 Cai, Y., Judd, K.L., & Lontzek, T.S., The Social Cost of Carbon with Economic and Climate Risks. http://arxiv.org/abs/1504.06909 (2015).

20 Nordhaus, W., Estimates of the Social Cost of Carbon: Concepts and Results from the DICE-2013R Model and Alternative Approaches. *Journal of the Association of Environmental and Resource Economists* 1 (1), 273-312 (2014).

21 Meinshausen, M. et al., The RCP greenhouse gas concentrations and their extensions from 1765 to 2300. Climatic Change 109, 213-241 (2011).

22 Epstein, L.G. & Zin, S.E., Substitution, risk aversion, and the temporal behavior of consumption and asset returns: a theoretical framework. *Econometrica* 57 (4), 937-969 (1989).

23 Pindyck, R.S. & Wang, N., The Economic and Policy Consequences of Catastrophes. *American Economic Journal: Economic Policy* 5 (4), 306-339 (2013).

24 Vissing-Jørgensen, A. & Attanasio, O.P., Stock-Market Participation, Intertemporal Substitution, and Risk-Aversion. *American Economic Review* 93 (2), 383-391 (2003).

25 Bansal, R. & Yaron, A., Risks for the Long Run: A Potential Resolution of Asset Pricing Puzzles. *The Journal of Finance* 59 (4), 1481-1509 (2004).

26 Barro, R.J., Rare Disasters, Asset Prices, and Welfare Costs. *American Economic Review* 99 (1), 243-264 (2009).

27 Nordhaus, W.D., Expert Opinion on Climatic Change. *American Scientist* 82, 45-51 (1994).

28 Nordhaus, W.D. & Boyer, J., *Warming the World. Models of Global Warming*. (MIT Press, Cambridge, Massachusetts, USA, 2000).

29 Baumol, W.J., On Taxation and the Control of Externalities. *The American Economic Review* 62 (3), 307-322 (1972).

30 Kopp, R.E. & Mignone, B.K., The U.S. Government's Social Cost of Carbon Estimates after Their First Two Years: Pathways for Improvement. *Economics: The Open-Access, Open-Assessment E-Journal* 6 (2012-15), 1-41 (2012).

31 Khan, S.A. *et al.*, Sustained mass loss of the northeast Greenland ice sheet triggered by regional warming. *Nature Clim. Change* 4 (4), 292-299 (2014).

32 Harig, C. & Simons, F.J., Accelerated West Antarctic ice mass loss continues to outpace East Antarctic gains. *Earth and Planetary Science Letters* 415 (0), 134-141 (2015).

33 Csatho, B.M. *et al.*, Laser altimetry reveals complex pattern of Greenland Ice Sheet dynamics. *Proceedings of the National Academy of Sciences* 111 (52), 18478-18483 (2014).

34 Bamber, J., van den Broeke, M., Ettema, J., Lenaerts, J., & Rignot, E., Recent large increases in freshwater fluxes from Greenland into the North Atlantic. *Geophysical Research Letters* 39 (19), L19501 (2012).

35 Peterson, B.J. *et al.*, Increasing river discharge to the Arctic Ocean. *Science* 298, 2171-2173 (2002).

36 Joughin, I., Smith, B.E., & Medley, B., Marine Ice Sheet Collapse Potentially Under Way for the Thwaites Glacier Basin, West Antarctica. *Science* 344 (6185), 735-738 (2014).

37 Rignot, E., Mouginot, J., Morlighem, M., Seroussi, H., & Scheuchl, B., Widespread, rapid grounding line retreat of Pine Island, Thwaites, Smith, and Kohler glaciers, West Antarctica, from 1992 to 2011. *Geophysical Research Letters* 41 (10), 3502-3509 (2014).

38 Wouters, B. *et al.*, Dynamic thinning of glaciers on the Southern Antarctic Peninsula. *Science* 348 (6237), 899-903 (2015).

39 Glotter, M.J., Pierrehumbert, R.T., Elliott, J.W., Matteson, N.J., & Moyer, E.J., A simple carbon cycle representation for economic and policy analyses. *Climatic Change* 126 (3-4), 319-335 (2014).

40 Bindoff, N.L. *et al.*, Detection and Attribution of Climate Change: from Global to Regional in *Climate Change 2013: The Physical Science Basis. Contribution of Working Group I to the Fifth Assessment Report of the Intergovernmental Panel on Climate Change*, edited by T.F. Stocker, D. Qin, G.-K. Plattner, M. Tignor, S.K. Allen, J. Boschung, A. Nauels, Y. Xia, V. Bex and P.M. Midgley (Cambridge University Press, Cambridge, United Kingdom and New York, NY, USA, 2013).

41 Rogelj, J. *et al.*, Energy system transformations for limiting end-of-century warming to below 1.5 [deg]C. *Nature Clim. Change* 5 (6), 519-527 (2015).

42 Rogelj, J. *et al.*, Zero emission targets as long-term global goals for climate protection. *Environmental Research Letters* 10 (10), 105007 (2015).

43 Nordhaus, W., *The Climate Casino: Risk, Uncertainty, and Economics for a Warming World*. (Yale University Press, 2013).

44 Anda, J., Golub, A., & Strukova, E., Economics of climate change under uncertainty: Benefits of flexibility. *Energy Policy* 37 (4), 1345-1355 (2009).

45 Martin, I.W.R. & Pindyck, R.S., Averting Catastrophes: The Strange Economics of Scylla and Charybdis. *American Economic Review* 105 (10), 2947-2985 (2015).

Correspondence and requests for materials should be addressed to t.m.lenton@exeter.ac.uk or lontzek@gmail.com

Acknowledgments. We thank Kenneth L. Judd and participants of the 2015 Annual Conference of the European Association of Environmental and Resource Economics for comments. Y.C. was supported by NSF (SES-0951576 and SES-1463644). T.S.L was supported by the Züricher Universitätsverein, the University of Zurich, and the Ecosciencia Foundation. T.M.L. was supported by a Royal Society Wolfson Research Merit Award and the European Commission HELIX project (ENV.2013.6.1-3). Supercomputer support was provided by Blue Waters (NSF awards OCI-0725070 and ACI-1238993, and the state of Illinois).

Author contributions. Y.C., T.M.L. and T.S.L. designed research, performed research, and wrote the paper.

Figure legends

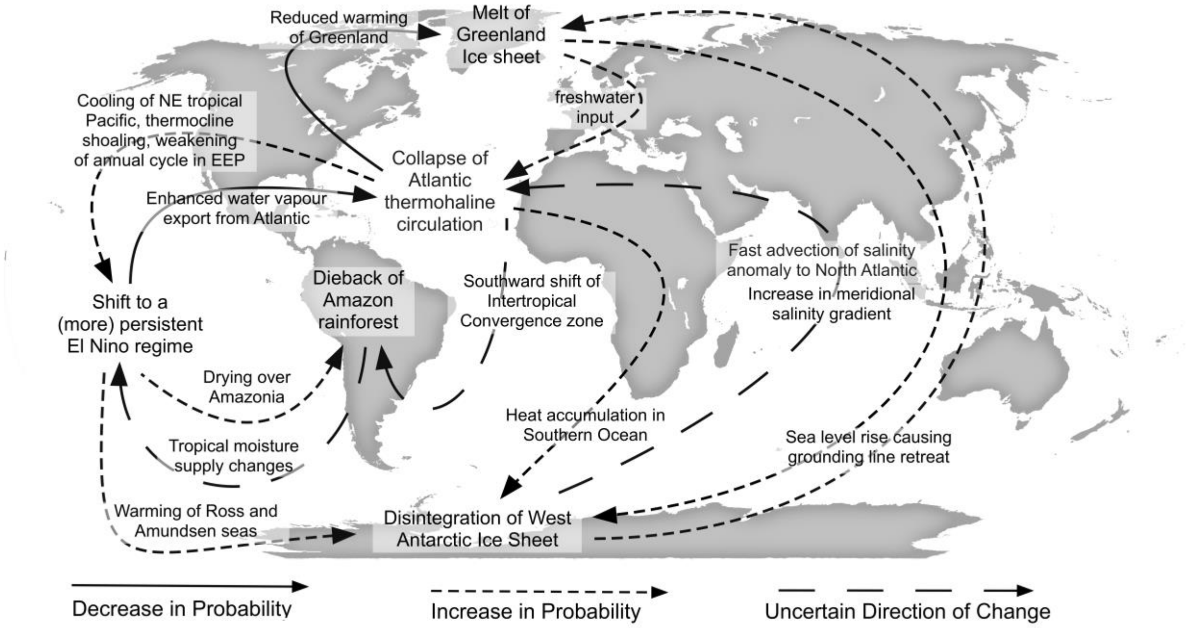

Figure 1. Map of the five climate tipping events considered here and the causal interactions between them previously identified in an expert elicitation[8].

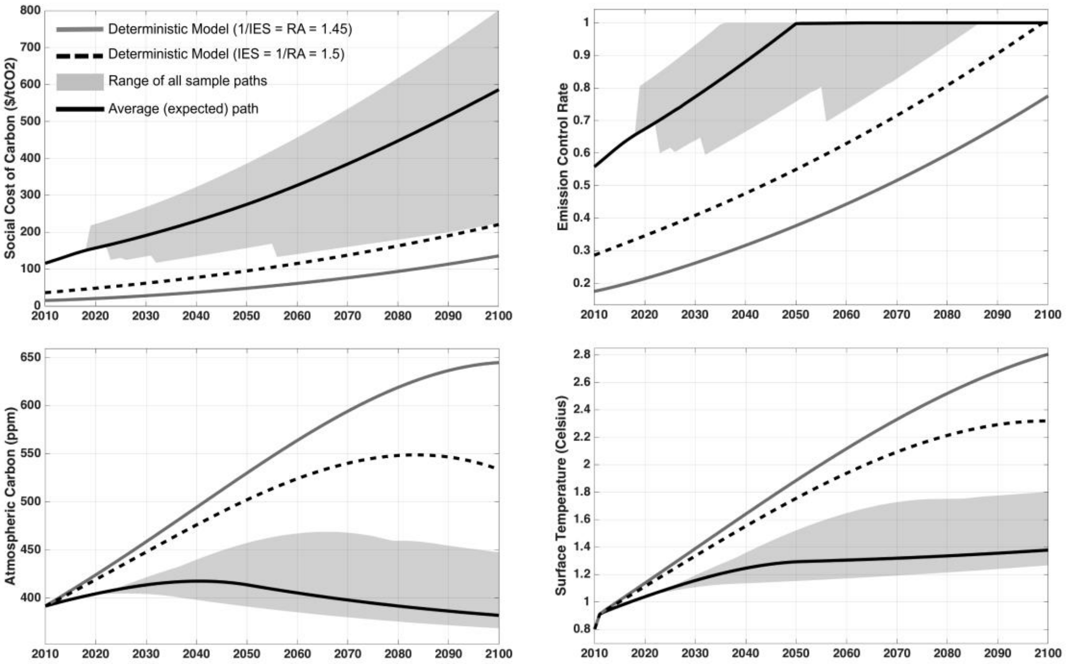

Figure 2. Results for: (a) the social cost of carbon, (b) emissions control policy, (c) atmospheric carbon (ppm), and (d) surface temperature change (above pre-industrial), in the baseline deterministic model (grey), the deterministic model with Epstein-Zin preferences (dashed black), and the expected path of stochastic model with multiple interacting tipping points (black). The grey-shaded area shows the range of sample paths from 10,000 simulations of the stochastic model (see Supplementary Figure 3 for the analogous case without interaction).

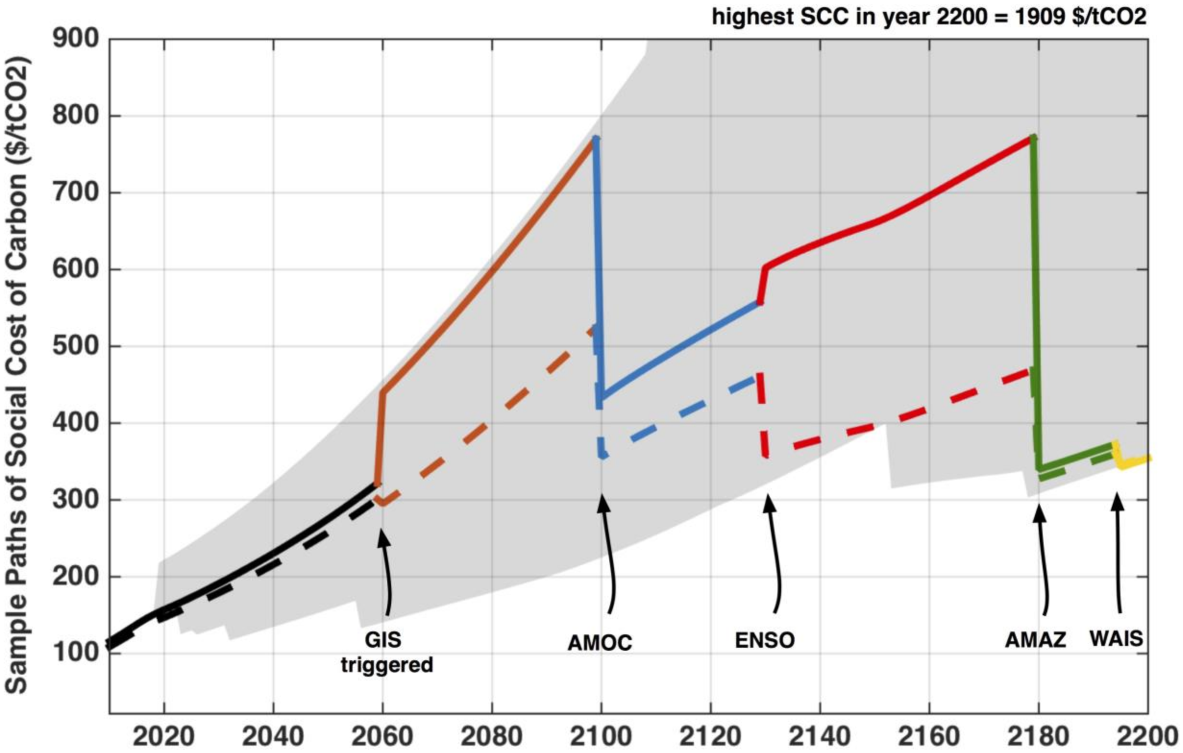

Figure 3. Example sample paths of the social cost of carbon (SCC) in $\$/\mathrm{tCO}_2$ with multiple tipping points interacting (solid line) and not interacting (dashed line) to highlight the effect of causal interactions between tipping events.

Tables

Table 1. Hazard rate, transition time, final damages and carbon cycle effect for each tipping element, with uncertainty ranges (in parentheses) considered in the sensitivity analysis.

Tipping element	Hazard rate (%/yr/K)	Transition time (years)	Final damages (% GDP)	Carbon cycle effect
AMOC	0.063	50 (10-250)	15 (10-20)	No effect
GIS	0.188	1500 (300-7500)	10 (5-15)	100 GtC over transition
WAIS	0.104	500 (100-2500)	5 (2.5-7.5)	100 GtC over transition
AMAZ	0.163	50 (10-250)	5 (2.5-7.5)	50 GtC over transition
ENSO	0.053	50 (10-250)	10 (5-15)	0.2 GtC/yr permanent

Table 2. Expected tipping point probabilities (%) by years 2100 and 2200, based on 10,000 model runs of the DSICE model[19] with five stochastic tipping points, and those that would be obtained from the temperature paths in the deterministic baseline model without tipping points, or under prescribed RCP 8.5 emissions.

Number of tipping events	**Stochastic tipping points (interacting)**		**Stochastic tipping points (no interaction)**		**Baseline model temperature path***		**RCP8.5 temperature path****	
	2100	**2200**	**2100**	**2200**	**2100**	**2200**	**2100**	**2200**
1	10.8	24.38	12.04	26.88	34.28	23.03	29.69	0
2	0.65	4.14	0.72	4.08	10.03	31.31	30.73	0
3	0.04	0.42	0.05	0.41	1.81	24.7	19.08	0.33
4	0	0.02	0	0.02	0.18	10.1	6.76	16.87
5	0	0.01	0	0	0	2.29	0.85	82.80
Cumulative probability	**11.49**	**28.97**	**12.81**	**31.39**	**46.30**	**91.43**	**87.11**	**100**

*2.8 °C warming in 2100, 2.76 °C in 2200

**4.7 °C warming in 2100, 7.5 °C in 2200

Methods

Summary

We use the DSICE model[10,19] (Supplementary Fig. 1) to compute the socially optimal reduction of global greenhouse gas emissions under the possibility of five interacting climate tipping points. The baseline deterministic model without tipping points is based on the 2013 version of DICE[20], but uses parameters in the carbon cycle and temperature system calibrated against all four RCP scenarios (see Supplementary Methods), and solves on an annual time step. DICE comprises one state variable for the capital stock, representing the world economy, a three-box carbon cycle module, and a two-box climate. To this we add a 10-dimensional system of interacting tipping elements.

For each of five tipping elements we have a discrete binary state indicating whether its corresponding tipping process has been already triggered or not, and a continuous state variable indicating the contemporaneous length of the transition process. The occurrence of each climate tipping point is modeled by a Markov process and its timing is not known at the times of decisions. The endogenous hazard rate (/yr/K) for each tipping event is assumed zero up to 1 °C warming above pre-industrial levels (reached in about 2015 in the model) and increases linearly with global warming above 1 °C at a rate derived from published expert elicitation results[8]. The conditional probabilities representing changes to the other hazard rates should a particular system tip are conservatively specified given wide ranges in the expert assessment[8]. The transition timescale[10] of each tipping element is based on current scientific understanding of the timescales at which specific climate subsystems can transition into an alternative state, with a factor of 5 uncertainty range in either direction considered in the sensitivity analysis. Tipping points are assumed to directly impact economic output and their relative final damages are based on scientific understanding. The absolute final damages of individual tipping events are highly uncertain and are varied in the sensitivity analysis over a factor of 2-3 range, giving a range in total reduction in GDP if all five tipping events occur of 23%-50%. In addition to the impacts of tipping points on economic output we also include conservative effects of tipping particular systems on the carbon cycle, implemented as exogenous emissions to the atmosphere. The stochastic model is solved using a supercomputer[19,46], to generate 10,000 stochastic sample paths, with the expected path calculated as the average of all paths.

In the following, we detail the specific modifications to the DICE-2013R model and refer to Nordhaus[43] for calibration and formulations of the remaining parts of the model.

Calibration of tipping elements and interactions between them

As in previous work[10] we define three phases to the tipping process for each tipping element (Supplementary Fig. 2). In the first, pre-trigger phase, the additional damage from a tipping point is 0. In the second, transition phase, there is a positive, but not stationary additional damage level. In the third and final, post-tipping phase the tipping element is in a new, absorbing state, with a constant (irreversible) damage level.

For each tipping element, i, after a tipping point is passed, a persistent climate impact state, the additional damage factor $J_{i,t}$ will increase continuously from a minimal level (i.e., $J_{i,t} = 0$) to some maximum level ($\overline{J_i} > 0$), implying that $J_{i,t+1} = \min\{J_{i,t} + \Delta_{i,t}, \overline{J_i}\} I_{i,t}$, where $\Delta_{i,t}$ is the incremental impact level from stage t to $t + 1$ of tipping element i . In our default case, $\Delta_{i,t}$ denotes linear increments, but these increments become nonlinear in the sensitivity case with endogenous transition time. We use $I_{i,t}$ as the indicator function to denote for each tipping element i the pre-trigger state of the world as $I_{i,t} = 0$ and the post-trigger state of the world as $I_{i,t} = 1$, where $I_{i,t}$ is a jump process with a Markovian hazard rate. The latter is endogenous with respect to the contemporaneous level of global average atmospheric temperature, T_t^{AT}. Furthermore, to model causal relationships between the tipping elements the Markovian hazard rate for tipping element i also depends on whether a tipping process of climate tipping element j has been triggered. We do not explicitly consider other indicators for tipping, e.g., the gradient of temperature[47]. The transition function for $I_{i,t}$ from stage t to stage $t + 1$ is $I_{i,t+1} = g_i^I(\boldsymbol{I_t}, T_t^{AT}, \omega_{i,t}^I)$, where $\boldsymbol{I_t}$ is the vector of the indicator functions for the five climate tipping elements $(I_{1,t}, \dots, I_{5,t})$ and $\omega_{i,t}^I$ is a random process. With $J_{i,t+1} = \min\{J_{i,t} + \Delta_{i,t}, \overline{J_i}\} I_{i,t}$ the impact factor on the economy becomes

$$\Omega_t\left({T_t}^{AT}, \boldsymbol{J_t}, \boldsymbol{I_t}\right) = \frac{\prod_i(1-I_{i,t}J_{i,t})}{1+\pi_2\left({T_t}^{AT}\right)^2} \tag{1}$$

where ${T_t}^{AT}$ is the average global atmospheric temperature and π_2 is a coefficient in the damage function. (The impact of global warming on the economy is reflected by a convex damage function of atmospheric temperature, which is a standard feature of the DICE model – a deterministic model specification would simply be to fix all $I_{i,t}$ at 0.) We specify the probability transition matrix of the tipping process i at time t as

$$\begin{bmatrix} 1 - p_{i,t} & p_{i,t} \\ 0 & 1 \end{bmatrix} \tag{2}$$

where its (n, m) element is the transition probability from state n to m for $I_{i,t}$, and $p_{i,t} = 1 - \exp(-B_i(\boldsymbol{I}) \max\{0, T_t^{AT} - 1\})$, where $B_i(\boldsymbol{I})$ is the hazard rate function for tipping element i, depending on whether other tipping elements have tipped. A general formula for the hazard rate function is given by

$$B_i(\boldsymbol{I}) = b_i \cdot (1 + \textstyle\sum_j (I_j \cdot f_{ij})). \tag{3}$$

We calibrated the values for b_i using the expert opinions reported in Kriegler et al.[8] and our previously described methodology[10]. Specifically, we calibrated b_i to match the average expert's cumulative trigger probabilities for each tipping element by the year 2200 for the medium temperature corridor in Kriegler et al.[8], which implies 2.5 °C warming in 2100 and 3 °C warming in 2200. These probabilities are 22% for AMOC, 52% for GIS, 34% for WAIS, 48% for AMAZ and 19% for ENSO. The corresponding values for b_i are b_{AMOC} = 0.00063064, b_{GIS} = 0.00188445, b_{WAIS} = 0.00103854, b_{AMAZ} = 0.00163443 and b_{ENSO} = 0.000526678 (Table 1).

To model the interaction component of tipping point likelihood, we introduce f_{ij} as an additional probability factor, which describes by how much the hazard factor for tipping element j is affected if tipping element i has tipped (when it is negative, it implies a decrease in probability). The parameter matrix f_{ij} is calibrated for $i, j \in \{$AMOC, GIS, WAIS, AMAZ, ENSO$\}$. Again we use the results in Kriegler et al.[8] as the source for our calibration of the interaction effects between tipping elements. In particular, we consider the core experts' assessment of the interaction effects for the "medium" temperature corridor. Our aim is to implement the interactions as direct, conditional alterations to the hazard rate of individual tipping events. Supplementary Table 1 summarizes our calibrated factors, f_{ij}. For some of the interaction effects, experts assessed ambiguous effects. For example, in the case of WAIS affecting AMOC the interaction factor ranges between <0 and >0 among the experts and among the average optimistic and pessimistic opinions of the core experts. In such an ambiguous case, while it might be worthwhile incorporating this uncertainty in the direction of interaction, we leave that as a possible avenue for further research and focus here, as in the non-ambiguous cases, solely on the average core experts' assessment.

The order of the tipping sequence is important for the overall impact of any individual tipping element, due to asymmetric causal relationships between some of the tipping events (Fig. 1, Supplementary Table 1). For example, when GIS tipping is triggered first, the likelihood of AMOC is increased, but if instead a tipping point in the AMOC is triggered first, the likelihood of GIS tipping is reduced.

Specification of transition times, final damages, and carbon cycle effects

In addition to calibrating the hazard rate (described above), we have to specify the transition time, final damage levels and the effect on the carbon cycle for each tipping element (Table 1). We base this on reviews of the literature, updated from previous work[7,11]. Recognising the scientific and economic uncertainties in these choices, the transition times are given a common factor of 5 range of uncertainty in either direction from default values, and the final damages are given a factor of 2-3 total uncertainty range. The values chosen are briefly justified as follows:

AMOC: Past abrupt climate changes linked to reorganisations of the AMOC have occurred in a decade or less, but future AMOC collapse in model simulations can take a couple of centuries. Hence we opt for a 50-year default transition time and 10-250 year range. The AMOC collapse is often viewed as the archetype of a climate catastrophe; hence we assign it the highest final damage (accepting that others will question this). Past studies with DICE have suggested a collapse of the AMOC might result in a 25-30% reduction in GDP comparable with the Great Depression[27,28]. However, when combined with other tipping events this could lead to excessively high damages, so we opt for a 15% GDP reduction with a range of 10-20%. We considered the potential for the AMOC collapse to reduce both ocean heat[48] and carbon[49,50] uptake. However quantitative estimates of these effects based on existing studies[48-50] suggest they are small, hence they are ignored here.

GIS: Irreversible meltdown of the Greenland ice sheet typically takes millennia in model simulations[51,52], but models are unable to explain the speed of recent ice loss[7]. To cover the uncertainty we opt for a default timescale of 1500 years, with a minimum timescale[7] of 300 years and an upper limit of 7500 years. The final damages from the GIS melt will largely be due to sea-level rise[7] of around 7 metres, which is roughly twice what can come from WAIS disintegration[53]. Hence we give the GIS twice the default final damages of the WAIS, noting that the spatial pattern of sea level rise will be greatest furthest away from each ice sheet (due to gravitational effects). As well as flooding low-lying cities and agricultural land, flooding of large areas of low-lying permafrost (especially in Siberia) could ultimately release large amounts of carbon[11]. We conservatively assume an exogenous emission of 100 GtC over the duration of the transition, which is only ~6% of the total permafrost carbon reservoir[54].

WAIS: The West Antarctic ice sheet is grounded largely below sea level and has the potential for more rapid disintegration than the Greenland ice sheet[7], ultimately leading to up to 3.3 metres sea-level rise[53]. Past sea-level rise in the penultimate Eemian inter-glacial period is estimated to have occurred[55] at rates >1 m/century and must have come from Antarctica and/or Greenland. We assign a minimum timescale of 100 years for WAIS disintegration, with a default setting of 500 years, and an upper limit of 2500 years. Noting that the effect of GIS meltdown on Arctic sea level is greatly suppressed by gravitational adjustment[56], whereas that of WAIS disintegration is not[53], we assign WAIS the same potential to release 100 GtC from low-lying permafrost over the duration of the transition.

AMAZ: Dieback of the Amazon rainforest in future model simulations[57] takes around 50 years, which we use as our default. However, if drought and corresponding fires respond very non-linearly to climate change[58] dieback could conceivably occur on a minimum timescale of 10 years, whereas if the forest is more resilient it could take centuries, consistent with a maximum timescale of 250 years. The Amazon rainforest is estimated to store 150-200 GtC in living biomass and soils[59] and we conservatively assume that dieback will release 50 GtC over the duration of the transition.

ENSO: In the past the frequency and amplitude of ENSO variability has changed on decadal to centennial timescales[7], and in the future the amplitude of ENSO variability is expected to increase with more frequent extreme El Niño and extreme La Niña events[60]. Past El Niño and La Niña events have had large impacts, especially on the agricultural sector, and their more global footprint than Amazon dieback leads us to assign higher damages to ENSO. The observational record shows that individual strong El Niño events can cause anomalous emissions of carbon by fire[61] of ~2 GtC. Hence we assume that an increase in El Niño amplitude could readily cause an average increase in land carbon emissions (exogenous) by 0.2 GtC/yr that is essentially permanent on the timescale of our integrations.

The combined effect on final damages if all tipping points occur is 38%, with a 23%-50% range in our sensitivity analysis. However, the timescale for all damages to be felt in our default case is over 1000 years, and our tipping probabilities are relatively low. Only two tipping elements (GIS, AMAZ) have an expected tipping time around 2200 (when it is as likely as not that their tipping process will be triggered), with the remaining three elements being less likely to tip. Furthermore, slow transition times mean that damages tend to be discounted away. As we have shown previously[10], a tipping point with 2.5% damage to GDP and a 5 year transition time will have much larger impact on the SCC today than a tipping point with 25% damage to GDP and a 500 year transition time. Other integrated assessment model studies that treat tipping points have tended to assume instantaneous transitions and double-digit percentage damages. Thus, we argue that overall our model is conservatively calibrated with relatively low expected damages, which amount to 0.53% of GDP in 2100 and 1.89% of GDP in 2200 in our default model parameterization.

The couplings to the carbon cycle lead to the following new specification of the exogenous land carbon source (in GtC) in DSICE:

$$\begin{aligned} E_{Land,t} = 0.9e^{-0.04t} \; & + I_{GIS} \cdot I\_\{J_{GIS} < \overline{J_{GIS}}\} \cdot \tfrac{100}{1500} \\ & + I_{WAIS} \cdot I\_\{J_{WAIS} < \overline{J_{WAIS}}\} \cdot \tfrac{100}{500} \\ & + I_{AMAZ} \cdot I\_\{J_{AMAZ} < \overline{J_{AMAZ}}\} \cdot \tfrac{50}{50} \\ & + 0.2\left(J_{ENSO}/\overline{J_{ENSO}}\right), \end{aligned} \tag{4}$$

where the first term on the right hand side is from the DICE model and all remaining terms are our modifications. Here, $I\_\{\}$ serves as an indicator function.

The Dynamic Programming Problem

In the following we present the dynamic programming problem of the social planner:

$$V_t(\boldsymbol{\mathcal{S}}) = \max_{C_t,\mu_t} u(C_t, L_t) + \beta\left[\mathbb{E}\left\{(V_{t+1}(\boldsymbol{\mathcal{S}}^+))^{\frac{1-\gamma}{1-1/\psi}}\right\}\right]^{\frac{1-1/\psi}{1-\gamma}} \tag{5}$$

$$s.t \quad K^+ = (1-\delta)K + Y_t(K, T^{AT}, \boldsymbol{I}, \boldsymbol{J}) - C_t - \Psi_t \tag{6}$$

$$\boldsymbol{M}^+ = \boldsymbol{\Phi}^M \boldsymbol{M} + (\mathcal{E}_t(K, \mu), 0, 0)^\top \tag{7}$$

$$\boldsymbol{T}^+ = \boldsymbol{\Phi}^T \boldsymbol{T} + (\xi_1 \mathcal{F}_t(M^{AT}), 0)^\top \tag{8}$$

$$I_i^+ = g_i(\boldsymbol{I}, T^{AT}, \omega_i) \tag{9}$$

$$J_i^+ = \min\{J_i + \Delta_i, \overline{J_i}\} I_i \tag{10}$$

where $V_t(\boldsymbol{S})$ denotes the time t value function which is endogenous in the 16-dimensional state vector denoted by $\boldsymbol{S}$. Furthermore, C_t, μ_t are the control variables for consumption and mitigation. Each period's utility u depends on consumption and exogenous labour supply L_t. With β we denote the utility discount rate. The expectation operator is over the next-period's value function with γ and ψ denoting the risk aversion parameter and the elasticity of inter-temporal substitution, respectively. In our default parameter case, we follow the calibration by Pindyck & Wang[23] and specify: $\gamma = 3.066$ and $\psi = 1.5$. Furthermore, $K, \boldsymbol{M}$ and $\boldsymbol{T}$ denote the capital stock, the three carbon stocks and the two temperatures (M^{AT} and T^{AT} represent carbon concentration and temperature in the atmosphere), respectively and a "+" superscript denotes a variable's next period value. Y_t denotes world gross product net of damages and $\mathcal{E}_t$ denotes non-mitigated emissions into the atmosphere. Finally Ψ_t is the expenditure on mitigation, and $\mathcal{F}_t$ is a term related to radiative forcing. The model is solved for the next 300 years with a terminal value function approximating the welfare of future years from 301 to infinite horizon (see Supplementary Methods). Our SCC is computed via

$$SCC_t = -1000\left(\frac{\partial V_t}{\partial M_t^{AT}}\right)/\left(\frac{\partial V_t}{\partial K_t}\right),$$

as in DSICE[19], denoting the marginal rate of substitution between atmospheric carbon concentration and capital.

After solving the dynamic programming problem using parallel backward value function iteration[46] (see Supplementary Methods), we use these approximated value functions V_t to simulate 10,000 paths in the following way: at the initial time, its state vector $\boldsymbol{S_0}$ is known as the observed market values, then we can get the optimal consumption and emission control rate at time 0 by solving the dynamic programming problem with the previously computed

V_1. Using sample realization of shocks, we can obtain the next state vector $\boldsymbol{S_1}$; using the same method to iterate forward, we get one simulated path of states and optimal policies that depend on realization of shocks. Repeating this process, we get 10,000 sample paths for our analysis.

Numerical Implementation of the Model

We have found that for the relatively short time horizon, when recalibrating the carbon cycle and temperature modules to match all four RCP scenarios closely we can omit the deep ocean stock of carbon without any loss of accuracy in the carbon-to-temperature relationship. Thus, the numerical implementation of the model is fifteen-dimensional. The computational task required to solve this fifteen-dimensional problem goes far beyond what has previously been achieved in truly stochastic climate-economy models, where 3-4 dimensional problems are considered the current frontier. We solve the model with parallel dynamic programming methods[46] on 312,500,000 approximation nodes for the 10-dimensional continuous state space and degree-4 complete Chebyshev polynomials for each of the 5 discrete state vectors. It takes about 3 hours to solve the model for a single set of parameter values on 10,560 cores at the Blue Waters supercomputer. The estimated error bound of the optimal solution is 0.1%-1% for policy functions and 0.01%-0.1% for the value functions.

Sensitivity analyses

We conducted several sensitivity analyses. Firstly we varied the transition times and/or damages of all five tipping elements across their assigned uncertainty ranges. Secondly we took a more pessimistic assessment of the interaction between the tipping elements (Supplementary Table 3), which uses the upper bounds of the core experts' assessment.

Thirdly, some more complex sensitivity studies were also conducted exploring the effect of endogenous transition times for tipping elements. In our model the transition time for tipping element i is inversely tied to $\Delta_{i,t}$, the annual damage increase during the transition phase. Thus, the transition time for element i is proportional to $\frac{1}{\Delta_{i,t}}$ and also its final damage level $\overline{J_i}$. In the case of an endogenous transition time, we let the annual damage increase be $\Delta_{i,t} = \overline{J_i}\exp(a_i T_t^{AT} - b_i)$, where a_i and b_i are parameters calibrated to result in $\overline{J_i}/\Delta_{i,t}$ to be the long transition time for $T_t^{AT} = 0$ and short transition time for $T_t^{AT} = 6$. Thus, the endogenous transition time is equal to $\int_0^\infty \exp(a_i T_t^{AT} - b_i) I_{i,t} I_-\left(J_{i,t} < \bar{J}_i\right) dt$.

As a general rule, transition timescales should be governed by the internal dynamical timescale(s) of the system in question, so it may not be appropriate to include a temperature dependence of the transition timescale for all tipping elements. However, endogenous transition times have some backing for the major ice sheets, where models[51,52], show that the rate of ice sheet meltdown depends on the amount by which a temperature threshold is exceeded.

Additional References

46 Cai, Y., Judd, K.L., Thain, G., & Wright, S.J., Solving Dynamic Programming Problems on a Computational Grid. *Comput. Econ.* 45 (2), 261-284 (2015).

47 E. Nævdal, E. & Oppenheimer, M., The Economics of the Thermohaline Circulation – A Problem with Multiple Thresholds of Unknown Location. *Resource and Energy*

Economics 29, 4:262–283 (2007).

48 Kostov, Y., Armour, K.C., & Marshall, J., Impact of the Atlantic meridional overturning circulation on ocean heat storage and transient climate change. *Geophysical Research Letters* 41 (6), 2108-2116 (2014).

49 Perez, F.F. *et al.*, Atlantic Ocean CO2 uptake reduced by weakening of the meridional overturning circulation. *Nature Geosci* 6 (2), 146-152 (2013).

50 Zickfeld, K., Eby, M., & Weaver, A.J., Carbon-cycle feedbacks of changes in the Atlantic meridional overturning circulation under future atmospheric CO2. *Global Biogeochemical Cycles* 22 (3), GB3024 (2008).

51 Huybrechts, P. & De Wolde, J., The Dynamic Response of the Greenland and Antarctic Ice Sheets to Multiple-Century Climatic Warming. *Journal of Climate* 12, 2169-2188 (1999).

52 Robinson, A., Calov, R., & Ganopolski, A., Multistability and critical thresholds of the Greenland ice sheet. *Nature Clim. Change* 2 (6), 429-432 (2012).

53 Bamber, J.L., Riva, R.E.M., Vermeersen, B.L.A., & LeBrocq, A.M., Reassessment of the Potential Sea-Level Rise from a Collapse of the West Antarctic Ice Sheet. *Science* 324 (5929), 901-903 (2009).

54 Tarnocai, C. *et al.*, Soil organic carbon pools in the northern circumpolar permafrost region. *Global Biogeochemical Cycles* 23 (2), GB2023 (2009).

55 Rohling, E.J. *et al.*, High rates of sea-level rise during the last interglacial period. *Nature Geoscience* 1, 38-42 (2008).

56 Mitrovica, J.X., Tamislea, M.E., Davis, J.L., & Milne, G.A., Recent mass balance of polar ice sheets inferred from patterns of sea-level change. *Nature* 409, 1026-1029 (2001).

57 Huntingford, C. *et al.*, Towards quantifying uncertainty in predictions of Amazon 'dieback'. *Philosophical Transactions of the Royal Society of London B: Biological Sciences* 363 (1498), 1857-1864 (2008).

58 Brando, P.M. *et al.*, Abrupt increases in Amazonian tree mortality due to drought–fire interactions. *Proceedings of the National Academy of Sciences* 111 (17), 6347-6352 (2014).

59 Feldpausch, T.R. *et al.*, Tree height integrated into pantropical forest biomass estimates. *Biogeosciences* 9 (8), 3381-3403 (2012).

60 Cai, W. *et al.*, ENSO and greenhouse warming. *Nature Clim. Change* 5 (9), 849-859 (2015).

61 van der Werf, G.R. *et al.*, Continental-Scale Partitioning of Fire Emissions During the 1997 to 2001 El Niño/La Niña Period. *Science* 303 (5654), 73-76 (2004).

Supplementary Information:

Supplementary Methods: Calibration for the Climate System

The DSICE model used in this study is based on the DICE-2013R model where the carbon cycle and temperature modules are represented by a three-box and a two-box model respectively. DICE-2013R uses five-year time steps and its carbon cycle and temperature modules are calibrated with one RCP scenario. Our DSICE model instead uses annual time steps and four RCP scenarios (RCP2.6, RCP4.5, RCP6, RCP8.5) to calibrate the parameters in the carbon cycle and temperature modules. For each RCP emission scenario, MAGICC provides their corresponding scenarios of carbon concentration and temperature in the atmosphere. We use this information to calibrate the parameters in our carbon cycle and temperature modules.

For each RCP emission scenario, we first use it as the input E_t to the carbon cycle, and then it outputs a path of carbon concentration in the atmosphere via

$$\boldsymbol{M}_{t+1} = \Phi^M M_t + (E_t, 0, 0)^\top$$

with the carbon cycle transition matrix

$$\boldsymbol{\Phi}^M = \begin{bmatrix} 1-\phi_{12} & \phi_{12} & 0 \\ \phi_{12} & 1-\phi_{21}-\phi_{23} & \phi_{32} \\ 0 & \phi_{23} & 1-\phi_{32} \end{bmatrix}$$

We calibrate the parameters in $\boldsymbol{\Phi}^M$ so that our generated paths of carbon concentration in the atmosphere match their corresponding RCP scenarios of carbon concentration in the atmosphere for all four RCP scenarios. Our numerical calibration shows that ϕ_{23} and ϕ_{32} are nearly zero, so we drop the carbon concentration in the deep ocean in our numerical implementation, and find that it has almost no impact on the solutions.

The carbon concentrations in the atmosphere generate radiative forcing:

$$F_t = \eta \log_2(M^{AT}/M_*^{AT}) + F_t^{EX},$$

where M_*^{AT} is the preindustrial carbon concentration in the atmosphere, and F_t^{EX} is exogenous radiative forcing. The radiative forcing impacts the surface temperature. With our carbon concentration paths, we have their corresponding radiative forcing scenarios. Using each of them as the input to the temperature system

$$\mathbf{T}_{t+1} = \mathbf{\Phi}^{\top}\mathbf{T}_t + (\xi_1 F_t, 0)^{\top},$$

with

$$\Phi^T = \begin{bmatrix} 1 - \varphi_{21} - \xi_2 & \varphi_{21} \\ \varphi_{12} & 1 - \varphi_{12} \end{bmatrix},$$

we can generate one path of surface temperature. We calibrate the parameters ξ_1, ξ_2, φ_{21}, φ_{12} so that our generated paths of surface temperature match the corresponding RCP scenarios of surface temperature for all four RCP scenarios.

Supplementary Methods: Economic System

In the economic system of DSICE, our utility at period t is

$$u(C_t, L_t) = \frac{(C_t/L_t)^{1-1/\psi}}{1-1/\psi} L_t \ ,$$

where C_t is consumption, ψ is IES (inter-temporal elasticity of substitution), and L_t is population (in billions) given as

$$L_t = 6.838e^{-0.0254t} + 10.5(1 - e^{-0.0254t})$$

The gross world output at year t is

$$Y_t(K_t, T_t^{AT}, \boldsymbol{I}_t, \boldsymbol{J}_t) = A_t K_t^{\alpha} L_t^{1-\alpha} \Omega_t\left(T_t{}^{AT}, \boldsymbol{J_t}, \boldsymbol{I_t}\right)$$

with

$$\Omega_t\left(T_t{}^{AT}, \boldsymbol{J_t}, \boldsymbol{I_t}\right) = \frac{\prod_i (1 - I_{i,t} J_{i,t})}{1 + \pi_2 \left(T_t{}^{AT}\right)^2}$$

defined in the main text. The mitigation expenditure is

$$\Psi_t = \theta_{1,t} \mu_t^{\theta_2} Y_t(K_t, T_t^{AT}, \boldsymbol{I}_t, \boldsymbol{J}_t)$$

Thus, the law of transition for capital K_t is

$$K_{t+1} = (1 - \delta) K_t + Y_t(K_t, T_t^{AT}, \boldsymbol{I}_t, \boldsymbol{J}_t) - C_t - \Psi_t$$

The carbon emission from economic activity and land is

$$\mathcal{E}_t(K_t, \mu_t) = \sigma_t(1 - \mu_t) A_t K_t^{\alpha} L_t^{1-\alpha} + E_t^{Land}$$

where E_t^{Land} is defined in the main text. The exogenous paths A_t, $\theta_{1,t}$, σ_t, and the parameter values for α, π_2, θ_2, δ follow DICE-2013R.

Supplementary Methods: Terminal Value Function

Welfare is usually defined over an infinite horizon, while DICE-2013R approximates it with a 300 years horizon for numerical implementation, as values after 300 years are discounted to be small. In the DSICE model, we use a terminal value function at the “terminal” time t=301 to approximate the welfare after 300 years, for a more precise numerical implementation and also a more stable value function iteration for solving the dynamic programming problem defined in the main text.

To compute the terminal value function, we assume that the emission control rate will always be one after 300 years, and consumption will always be 0.74 share of gross world production. If one tipping element has been tipped before the terminal time, then its damage will keep unfolding, otherwise we assume it will never be tipped after the terminal time. We assume that all exogenous paths will stop changing after the terminal time. Under these assumptions, for any terminal state $\boldsymbol{\mathcal{S}}$, we can generate a flow of consumption after the terminal time, and then we estimate the value of the terminal value function at that state to be

$$V_{301}(\boldsymbol{\mathcal{S}}) = \sum_{t=301}^{\infty} e^{-\rho(t-301)} u(C_t, L_t)$$

For the numerical implementation, we compute the above summation over 400 years (i.e., from year 301 to 700) as an approximation. Our numerical examples show that solutions for the first 200 years are insensitive to the choice of the terminal value function, due to the discounted effect inherent in the DICE-2013R model, but the terminal value function specified above is still essential because it enables us to have stable value function iteration.

Supplementary Methods: The Numerical Algorithm

We use parallel backward value function iteration[46] to solve the dynamic programming problem (5)-(10). With the above defined terminal value function V_{301}, for a state $\boldsymbol{\mathcal{S}}$ at time t=300, we use an optimization solver to solve the dynamic programming problem and then get $V_{300}(\boldsymbol{\mathcal{S}})$. Since this is a problem with both continuous and discrete state variables, we cannot compute $V_{300}(\boldsymbol{\mathcal{S}})$ for all possible states $\boldsymbol{\mathcal{S}}$. Instead we choose a set of approximation state nodes $\boldsymbol{\mathcal{S}}_{\boldsymbol{i}}$ and compute $v_i = V_{300}(\boldsymbol{\mathcal{S}}_{\boldsymbol{i}})$, and then use a complete Chebyshev polynomial to approximate the value function V_{300} at continuous state variables for each discrete state vector, so that $v_i \approx V_{300}(\boldsymbol{\mathcal{S}}_{\boldsymbol{i}})$, but now we have a value of V_{300} at any state $\boldsymbol{\mathcal{S}}$**.** Note that these optimization problems are naturally parallelizable. Iterating backwards from t=300 to t=0, we get all value functions V_t and also their corresponding policy functions. Using these value functions, we can then iterate forward to get one simulated path of optimal policies which depend on realization of the shocks, and repeat it to obtain 10,000 simulation paths, as described in the main text. See refs. [19,46] for more detailed discussion.

Supplementary Tables

Supplementary Table 1. Interaction terms between tipping events (f_{ij}), which describe by how much the hazard factor for tipping element j is affected if tipping element i has tipped.

Tipping element *i*	Tipping element *j*				
	AMOC	GIS	WAIS	AMAZ	ENSO
AMOC		-0.235	0.125	0.55	0.121
GIS	1.62		0.378	0.108	0
WAIS	0.107	0.246		0	0
AMAZ	0	0	0		0
ENSO	-0.083	0	0.5	2.059	

Supplementary Table 2. Sensitivity analysis for simultaneously varying the transition times and damages of all five tipping elements.

Social cost of carbon in 2010 (\$/tCO$_2$)	High damage	Default damage	Low damage
Short transition time	166	145	94
Default transition time	145	116	77
Long transition time	75	62	50

Supplementary Table 3. Pessimistic assessment of the interaction terms between tipping events (f_{ij}) using the upper bounds of the core experts' assessment.

Tipping element *i*	Tipping element *j*				
	AMOC	GIS	WAIS	AMAZ	ENSO
AMOC		-0.056	0.25	1	0.25
GIS	3.04		0.68	0.2	0
WAIS	0.44	0.483		0	0
AMAZ	0	0	0		0
ENSO	0.16	0	1	3.83	

Supplementary Figures

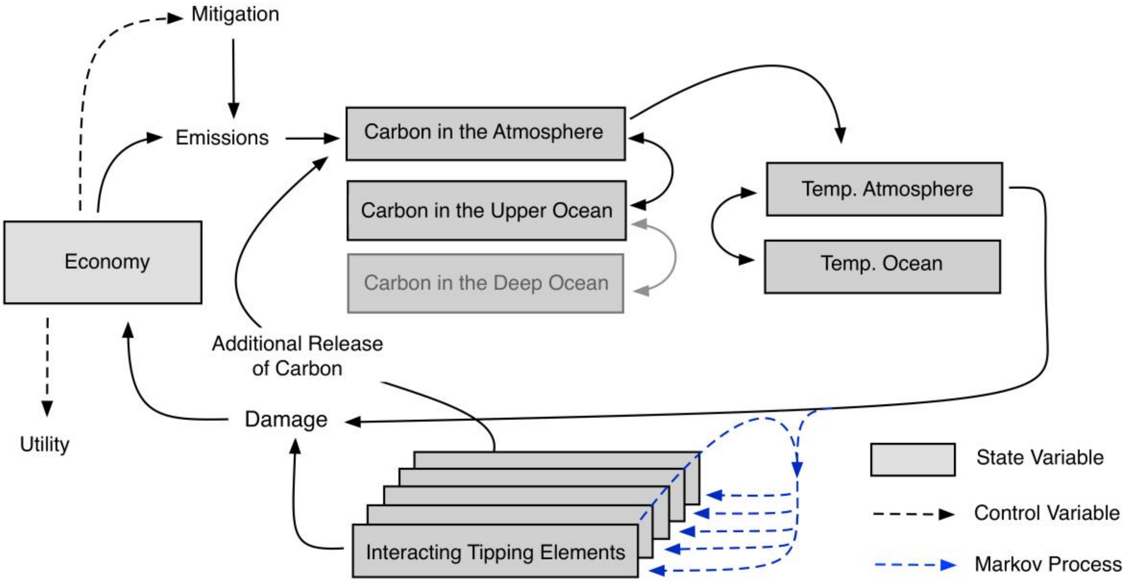

Supplementary Figure 1. Schematic of the DSICE model used in this study. The "deep ocean carbon" box is shaded as it can be omitted in the numerical analysis (see "Numerical Implementation of the Model" in the Methods section).

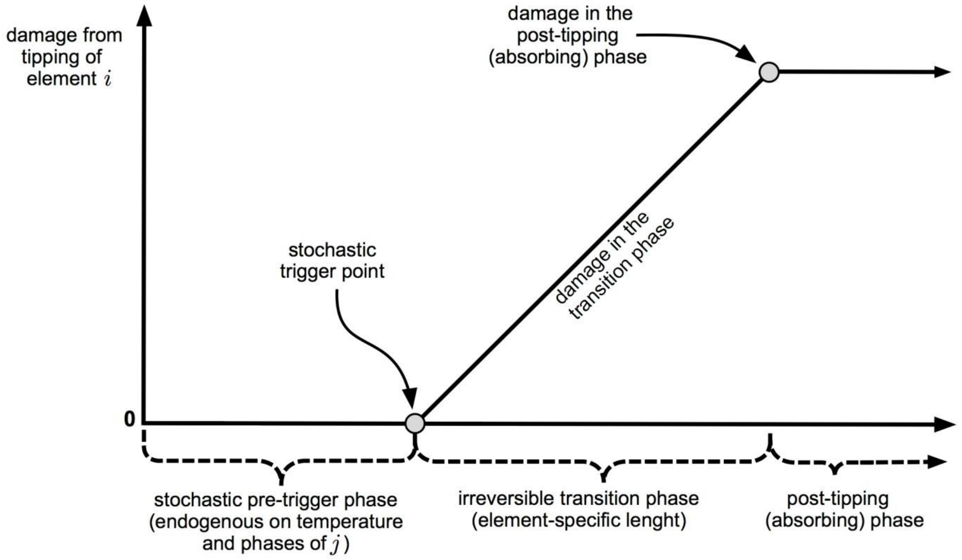

Supplementary Figure 2. Schematic of the tipping process in the DSICE model.

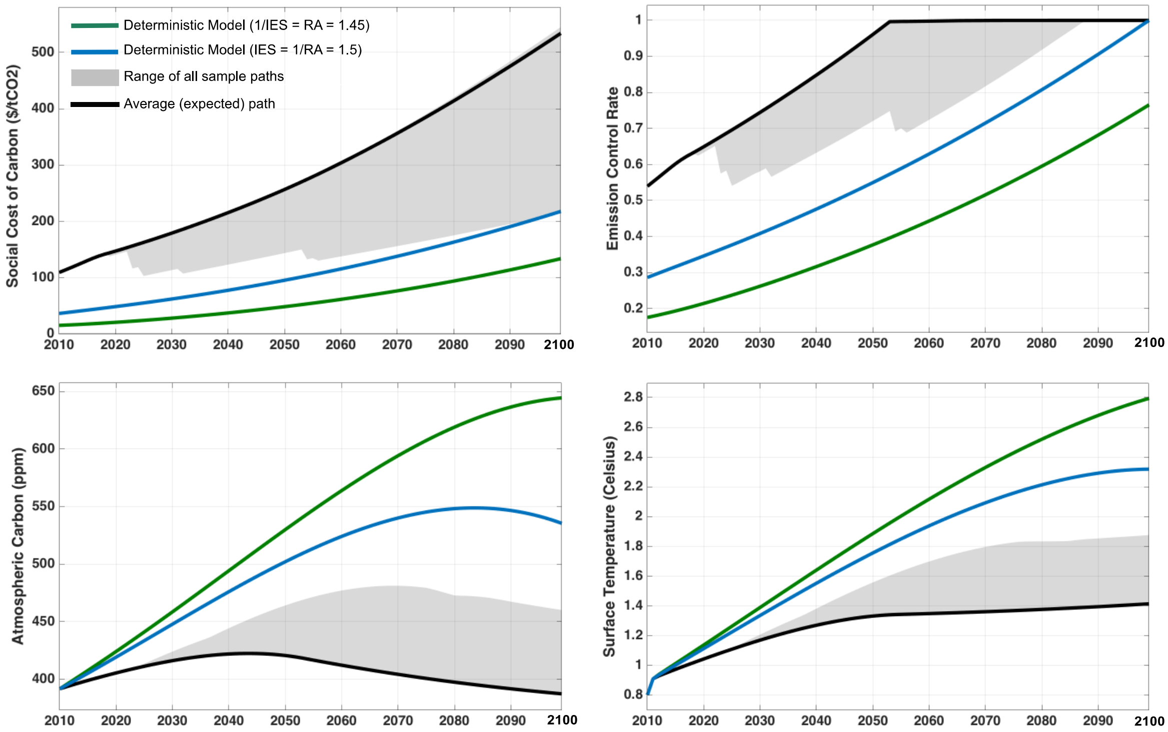

Supplementary Figure 3. Results for: (a) the social cost of carbon, (b) emissions control policy, (c) atmospheric carbon (ppm), and (d) surface temperature change (above pre-industrial), in the baseline deterministic model (green), the deterministic model with Epstein-Zin preferences (blue), and the expected path of stochastic model with multiple tipping points (black) in case without interaction. The grey-shaded area shows the range of sample paths from 10,000 simulations of the stochastic model (see Figure 2 for the analogous case with interaction).

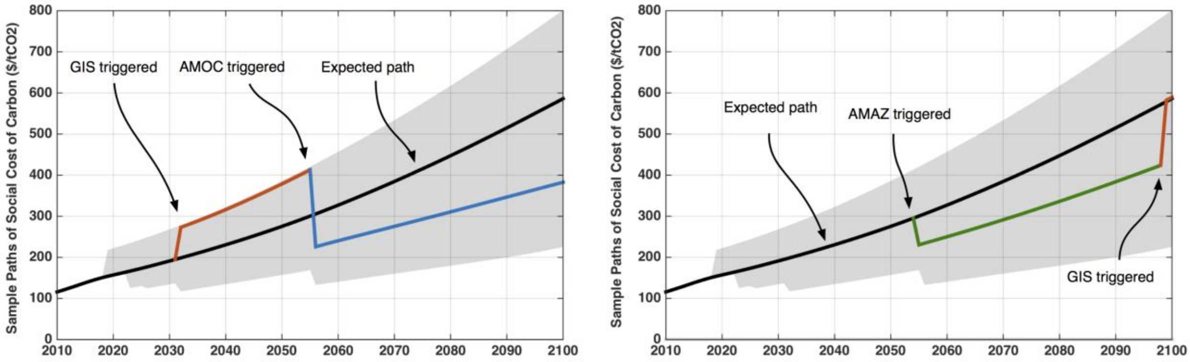

Supplementary Figure 4. Example sample paths with two tipping events this century.

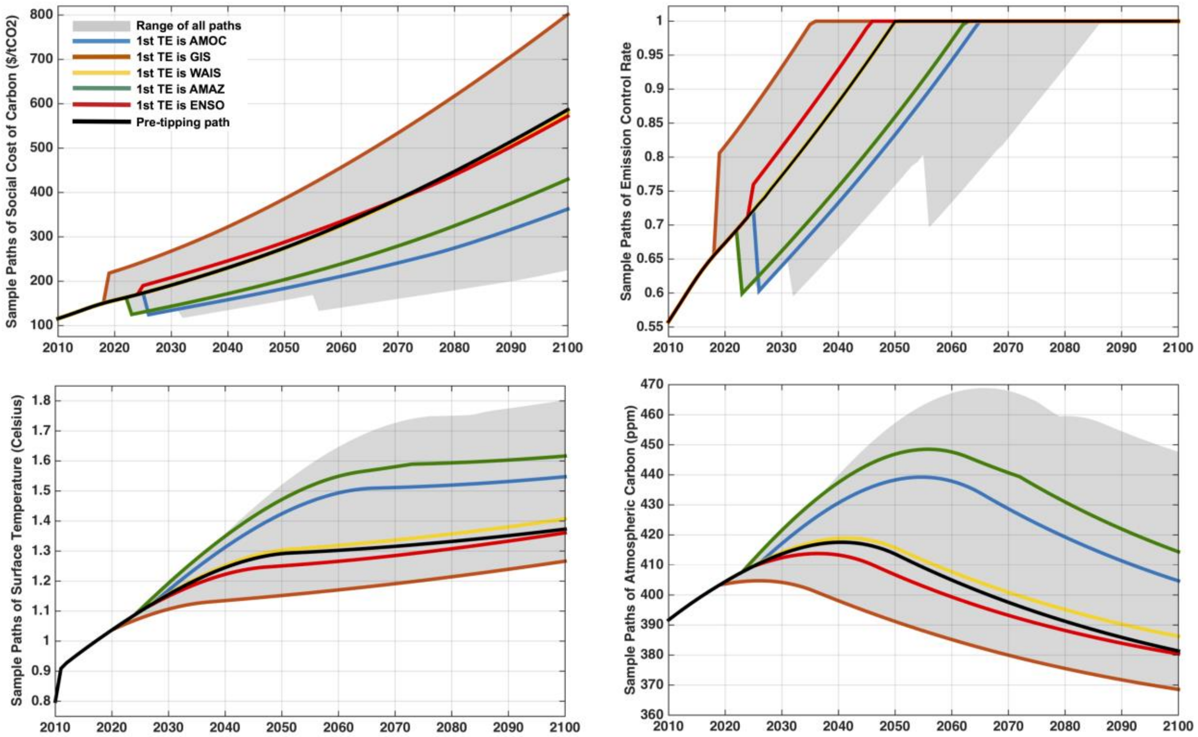

Supplementary Figure 5. Sample paths of the earliest (and sole) tipping of each element.

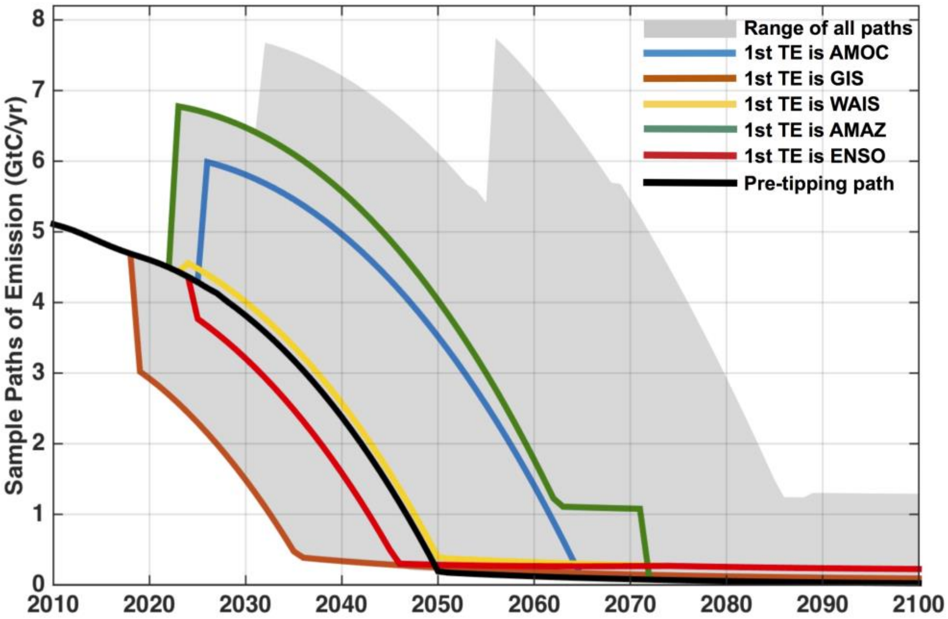

Supplementary Figure 6. Sample emission paths of the earliest (and sole) tipping of each element.